Journal of Hazardous Materials 192 (2011) 186–191

Contents lists available at ScienceDirect

Journal of Hazardous Materials

journal homepage: www.elsevier.com/locate/jhazmat

Photocatalytic activities of Mo-doped Bi_2WO_6 three-dimensional hierarchical microspheres

Xu Chun Song [a,*], Yi Fan Zheng [b], Rong Ma [a], Yao Yuan Zhang [a], Hao Yong Yin [c]

[a] Department of Chemistry, Fujian Normal University, Fuzhou 350007, PR China
[b] College of Chemical Engineering & Materials Science, Zhejiang University of Technology, Hangzhou 310014, PR China
[c] Institute of Environmental Science and Engineering, Hangzhou Dinazi University, Hangzhou 310018, PR China

ARTICLE INFO

Article history:
Received 13 February 2011
Received in revised form 10 April 2011
Accepted 1 May 2011
Available online 25 May 2011

Keywords:
Photocatalytic
Doping
Hydrothermal
Bi_2WO_6

ABSTRACT

The Mo-doped Bi_2WO_6 three-dimensional (3D) hierarchical microspheres from nanoplates have been synthesized by a hydrothermal route. The products were characterized in detail by multiform techniques: X-ray diffraction (XRD), energy-dispersive X-ray analysis (EDS), scanning electron microscopy (SEM), and UV–vis absorption spectrum. The results of the photocatalytic degradation of Rhodamine-B (RhB) in aqueous solution showed that molybdenum ions doping greatly improved the photocatalytic efficiency of Bi_2WO_6 3D hierarchical microspheres. The Mo-doped Bi_2WO_6 microspheres with atomic ratio of Mo–W of 0.05 had the best activity in photodegradation of RhB in aqueous solution under 500 W Xe lamp light irradiation.

1. Introduction

Water is a prime source for all living organism including human beings. Wastewater containing dyes coming from dyeing and finishing industry is generally high in both color and organic content. Their release as wastewater in the ecosystem is a dramatic source of esthetic pollution, eutrophication, and perturbations in aquatic life. Therefore, decolorization of wastewater from textile effluents has been the target of great attention in the last few years [1,2]. Oxide semiconductor photocatalysis has been extensively investigated since Honda and Fujishima discovered the photocatalytic splitting of water on TiO_2 electrodes in 1972 [3]. TiO_2 was intensively investigated because of its high activity, good photostability, low price, and non-toxicity. Many persistent organic substances were degraded in TiO_2 suspensions [4,5]. However, TiO_2 is a wide band gap semiconductor, which necessitates the use of mainly ultraviolet irradiation [6]. Slow reaction rate and poor solar efficiency (maximum 5%) have hindered the commercialization of this technology [7]. Thus, exploitation of a new photocatalyst system is compulsory. Tungstate materials, such as $CdWO_4$, $ZnWO_4$, $CoWO_4$ and $MnWO_4$ are known for their wide applications in conventional catalysis, or as scintillator material, in photoluminescence, optical fibres and as materials in microwave technology [8–11]. Due to their unique combination of physical and chemical properties, in terms of molecular and electronic versatility, reactivity, and stability, it is reasonable to believe they may be a promising class of photocatalysts.

Bi_2WO_6, a kind of multicomponent oxide, is one of the simplest Aurivillius oxides possessing a layered structure. It has been found to possess interesting physical properties such as ferroelectric, piezoelectricity, pyroelectricity, catalytic behavior, oxide anion conducting, luminescent properties and a nonlinear dielectric susceptibility [12–14]. Recently, visible-light-induced Bi_2WO_6 photocatalyst has been successfully synthesized via a facile low temperature combustion synthesis method, using glycine as the fuel [15]. Zhu et al. have reported fabrication of nanosized Bi_2WO_6 by a hydrothermal crystallization process. The further experiments revealed that Bi_2WO_6 photocatalyst was active for the RhB decomposition in the wide wavelength range, including both UV and visible-light [16]. Zeng et al. have reported the high photocatalytic capability of quantum dots modified Bi_2WO_6 nanostructures [17]. Previous studies indicated that the photocatalytic activity of catalysts depended strongly on two factors: adsorption behavior and the separation efficiency of electron-hole pairs. The adsorption capacity can be generally improved by increasing the specific surface area of catalysts. On the other hand, in order to eliminate the recombination rate of the electron-hole pairs, metals ions doping have been proposed [18]. Hence, many efforts have been made to synthesize nanosized Bi_2WO_6 to improve its photocatalytic activity [19,20]. However, the investigation on the photocatalytic activity of metal ion doped Bi_2WO_6 has never been reported before. Furthermore, it is difficult to separate and recycle nanoscale photocatalysts

* Corresponding author. Tel.: +86 591 87441126; fax: +86 591 83465376.
E-mail address: songxuchunfj@163.com (X.C. Song).

0304-3894/$ – see front matter © 2011 Elsevier B.V. All rights reserved.
doi:10.1016/j.jhazmat.2011.05.001

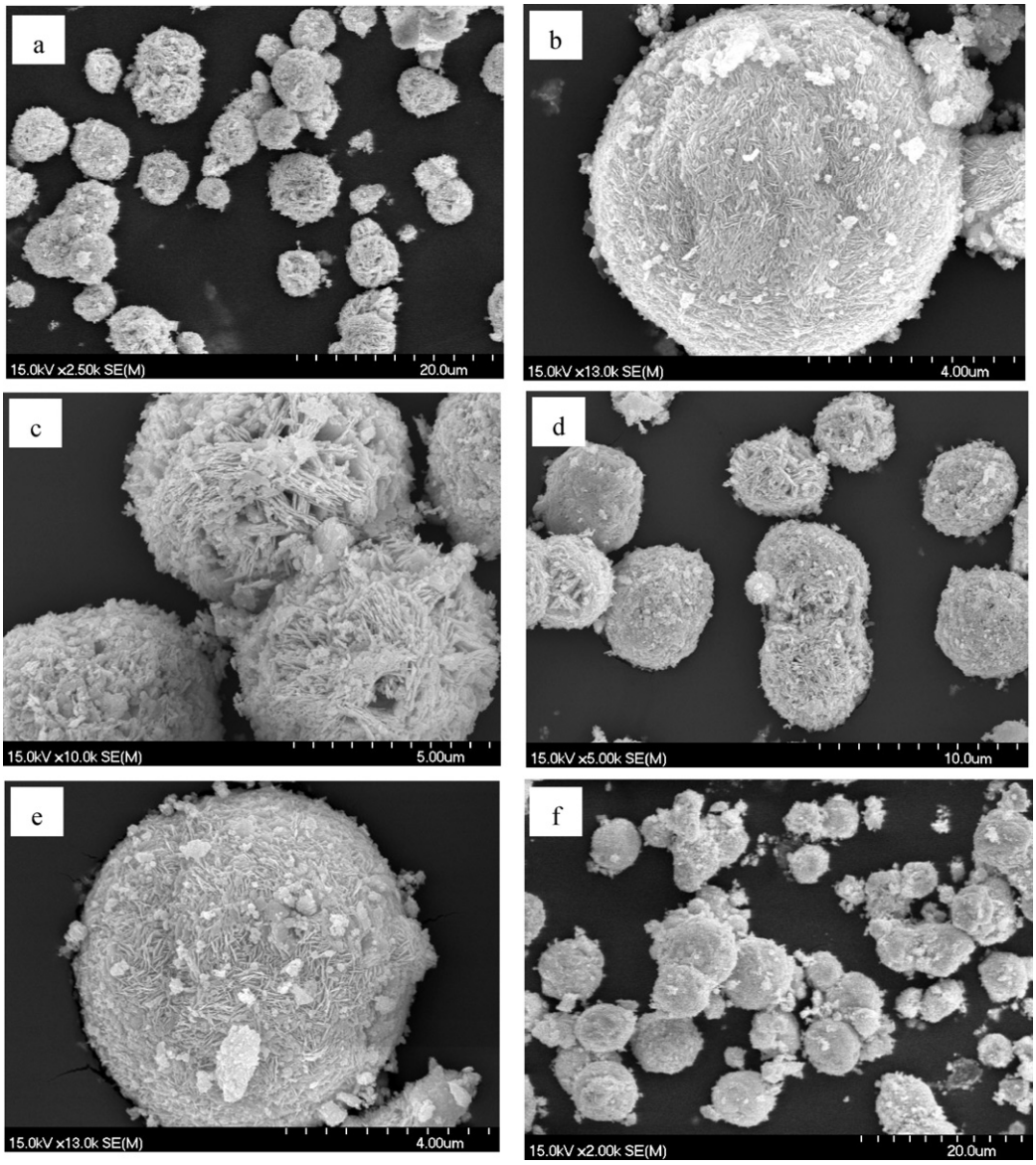

Fig. 1. SEM images of the Bi_2WO_6 hierarchical microspheres doped with different contents of molybdenum ions. The doping ratio of Mo/W was 0 (a and b), 0.02 (c), 0.05 (d and e), and 0.08 (f), respectively.

at present. Comparatively speaking, 3D microscale architectures fabricated from nanosized building blocks hold many advantages, such as high photocatalytic activity, abundant transport paths for small organic molecules, and comparative ease of separation and recyclability [21]. In this work, we report the synthesis of Mo-doped Bi_2WO_6 3D hierarchical microspheres by a hydrothermal method without using any templates or surfactants. The photocatalytic activities of the as-prepared samples for the Rhodamine-B (RhB) photodegradation were investigated. To further understand the mechanism of Mo-doped Bi_2WO_6 3D hierarchical photocatalysis, the effects of Mo-doping concentrations on the photocatalytic activity were discussed.

2. Experimental

2.1. Fabrication of Mo-doped Bi_2WO_6 3D hierarchical microspheres

All the chemicals were analytic grade reagents without further purification. Mo-doped Bi_2WO_6 3D hierarchical microspheres were synthesized under hydrothermal conditions. Experimental details were as follows: 4 mmol of $Na_2WO_4{\cdot}2H_2O$ and $(NH_4)_6Mo_7O_{24}{\cdot}4H_2O$ (the atomic ratios of Mo–W = 0, 0.02, 0.05, and 0.08) were dissolved in 45 mL deionized water to form a transparent solution. Then 8 mmol of $Bi(NO_3)_3{\cdot}5H_2O$ was added to the above solution under continuous stirring. The resulting suspension was transferred into a 50 mL Teflon-lined stainless steel autoclave. Hydrothermal treatments were carried out at 180 °C for 12 h. After that, the autoclave was allowed to cool down naturally. Precipitates were collected and washed with deionized water several times and dried in air at 100 °C. For convenience of description, changing the atom ratio of Mo–W, the 0.00, 002, 0.05 and 0.8 doping of molybdenum ions in Bi_2WO_6 hierarchical microspheres were marked as samples A, B, C and D, respectively.

2.2. Characterization

The morphologies were characterized using scanning electron microscopy (SEM, Hitachi S-4700, 25 kV) and transmission electron microscopy (TEM, Tecnai G2 F30 S-Twin, 200 kV). The

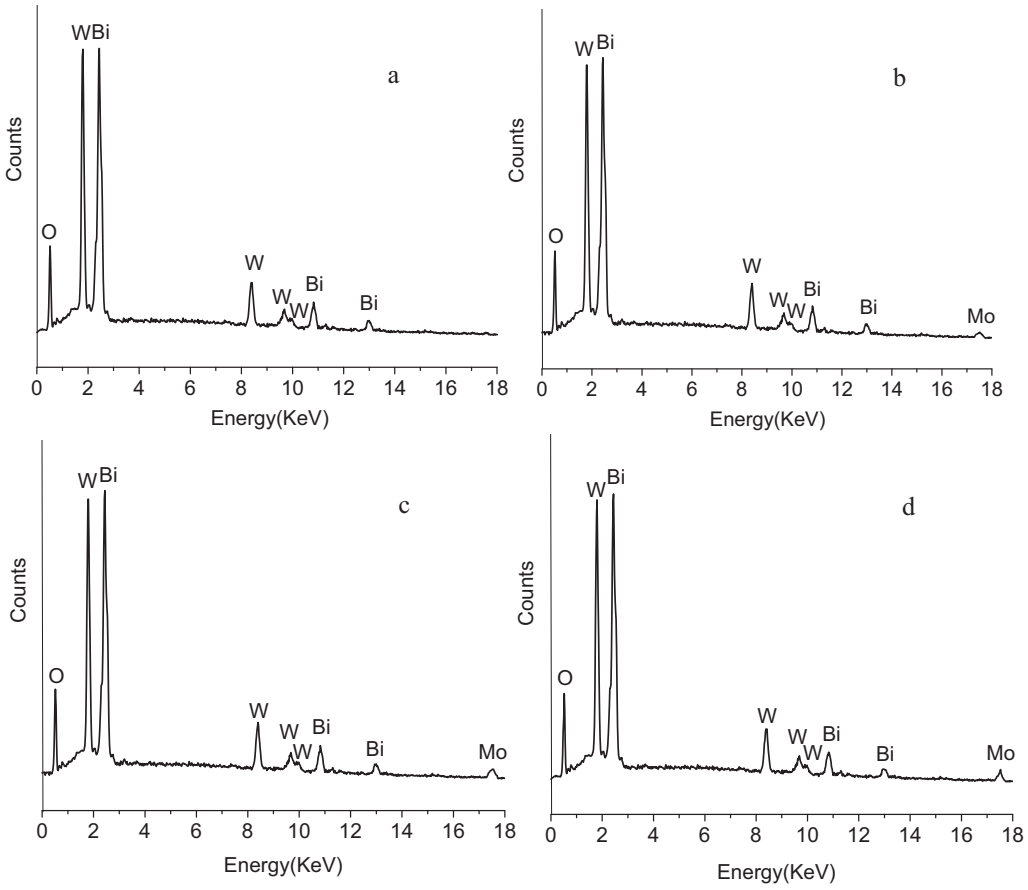

Fig. 2. EDS patterns of the Bi_2WO_6 hierarchical microspheres doped with different contents of molybdenum ions. From (a)–(d), the doping ratio of Mo/W was 0, 0.02, 0.05 and 0.08, respectively.

composition of the product was analyzed by energy dispersive X-ray detector (EDS, Thermo Noran VANTAG-ESI) and inductively coupled plasma (ICP, Autoscan Advantage, USA). The X-ray diffraction (XRD, Thermo ARL SCINTAG X'TRA with CuKα irradiation, $\lambda = 0.154056$ nm) was used to analysis the crystallinity. BET surface areas were measured by nitrogen adsorption at 77 K using a Micromeritics ASAP 2000 surface area analyzer. UV–visible diffuse reflectance spectra (UV–vis DRS) were obtained using a Hitachi U-3010 spectrophotometer. $BaSO_4$ was the reference sample, and the spectra were recorded in the range 200–600 nm.

2.3. Photocatalytic experiments

The photoactivity experiments on the samples for the photodegradation of RhB were performed at ambient temperature. Light source was a 500 W Xe lamp. In a typical process, aqueous suspensions of RhB (150 mL, $C_0 = 1 \times 10^{-5}$ M) and 100 mg of Mo-doped Bi_2WO_6 3D hierarchical microspheres were placed in a vessel. Prior to irradiation, the suspensions were magnetically stirred in the dark for ca. 30 min to ensure the equilibrium of the working solution. The suspensions were kept under constant air-equilibrated conditions before and during the irradiation. Analytical samples (3 mL) were drawn from the reaction suspension every 10 min, and removal of Mo-doped Bi_2WO_6 3D hierarchical microspheres by centrifugation. The changes of absorptions at wavelength 550 nm were applied to identify the concentrations of RhB using a 721-type spectrophotometer. The percentage of degradation is reported as C/C_0. C is the concentration of RhB for each irradiated time interval. C_0 is the initial concentration of RhB when adsorption/desorption equilibrium was achieved. To test its photocatalytic lifetime, Mo-doped Bi_2WO_6 3D hierarchical microspheres was recycled and reused five times in the decomposition of RhB under the same conditions. After each photocatalytic reaction, the aqueous solution was centrifuged to recycle Mo-doped Bi_2WO_6 3D hierarchical microspheres that were then dried at 100 °C for another test.

3. Results and discussion

The morphology and particle sizes of the Mo-doped Bi_2WO_6 with different contents of molybdenum ions were investigated by SEM. Fig. 1a describes the typical panoramic SEM image of pure Bi_2WO_6 (A). As can be seen from a low magnification SEM image, the sample consists of a large quantity of microspheres with diameters ranging between 4 and 8 μm. The surfaces of these microspheres are coarse and have many microstructures on them. An amplified SEM image of an individual microsphere indicates that the microsphere consists of many square nanoplates (Fig. 1b). Interestingly, when samples prepared at different Mo-doping concentrations (Fig. 1c–f), Mo-doped Bi_2WO_6 3D hierarchical microspheres can be obtained in the whole concentrations range under the investigation (Mo/W: 0.02–0.08). It was found that the Mo-doping concentration had little effect on the shape of products during this range. For example, SEM images of the Mo-doped Bi_2WO_6 3D hierarchical microspheres (*C*) are shown in Fig. 1d and e. Clearly, morphology and particle sizes of the Mo-doped Bi_2WO_6 microspheres were consistent with pure Bi_2WO_6.

Energy dispersive spectrometry (EDS) analysis was employed to determine the composition of the Mo-doped Bi_2WO_6 3D hierarchical microspheres. The EDS patterns of the Bi_2WO_6 3D hierarchical microspheres doped with different contents of molybdenum ions

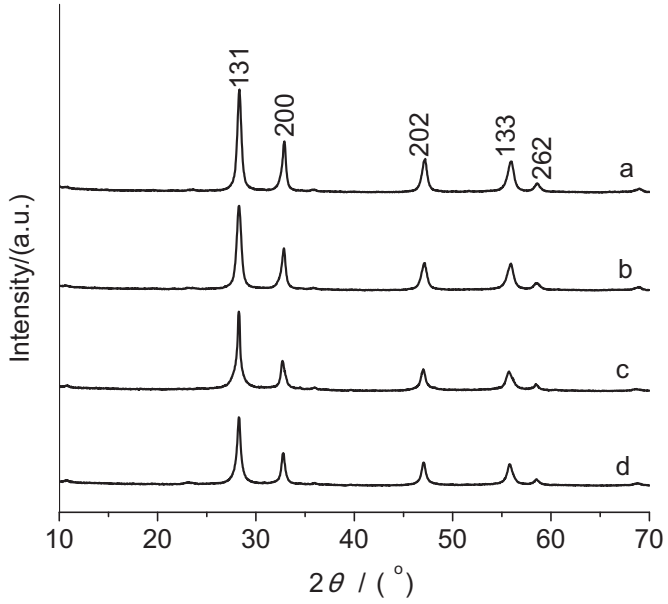

Fig. 3. XRD patterns of the Bi_2WO_6 hierarchical microspheres doped with different contents of molybdenum ions. From (a)–(d), the doping ratio of Mo/W was 0, 0.02, 0.05 and 0.08, respectively.

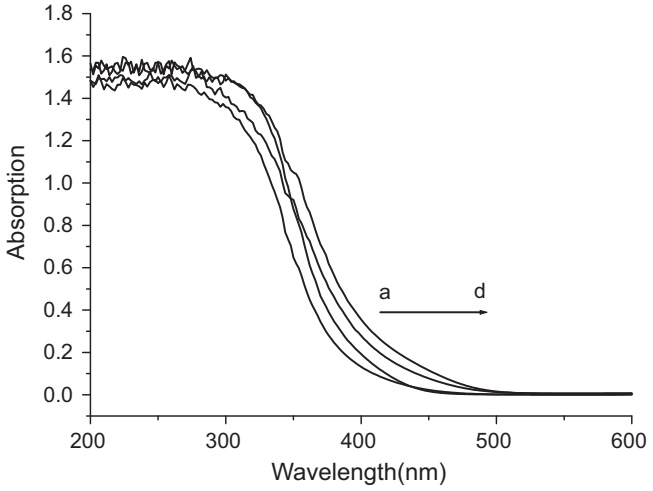

Fig. 5. UV–vis spectra of the Bi_2WO_6 hierarchical microspheres doped with different contents of molybdenum ions. From (a)–(d), the doping ratio of Mo/W was 0, 0.02, 0.05 and 0.08, respectively.

are shown in Fig. 2. With Mo-doping concentration increasing, the Mo peak intensity slightly increased. The results from EDS confirm that the obtained products are composed of the Bi_2WO_6 doped with molybdenum ions. ICP analysis was also employed to accurately determine the elemental content of the as-prepared samples. Mo and W elements exist in the Bi_2WO_6 and Mo-doped Bi_2WO_6 3D hierarchical microspheres with the Mo/W molar ratio of 0:100, 1.79:100, 4.83:100 and 7.91:100, respectively, which is close to the expected value in the experiment.

The crystallinity and phase purity of the products were examined by XRD measurement. Fig. 3 shows the XRD patterns of Mo-doped Bi_2WO_6 3D hierarchical microspheres with different contents of molybdenum ions. All of reflections can be indexed to orthorhombic-phase Bi_2WO_6, which is in good agreement with the reported data (JCPDS No. 39-0256). It is worth mentioning that the more the molybdenum ions doped, the narrower and lower was the diffraction spectrum as shown in Fig. 1b–e, which demonstrated that with the presence of molybdenum ions, the crystallization of the Bi_2WO_6 3D hierarchical microspheres was inhibited. It is interesting to note that there is no changes in the positions of diffraction peaks and there is no other phases been detected in the XRD patterns of the samples. One probable reason is that the structure of Mo^{6+} and W^{6+} ions are very similar and Bi_2WO_6 and Bi_2MoO_6 are Aurivillius structure, so the molybdenum ions may be easy to insert into the structure of Bi_2WO_6.

To further understand the detailed structural of the Bi_2WO_6 3D hierarchical microspheres doped with different contents of molybdenum ions, the high resolution TEM (HRTEM) technique was employed. Fig. 4a is a typical HRTEM image of pure Bi_2WO_6 with clear lattice fringes which shows the high crystallinity of the samples. However, in the HRTEM image of the Mo-doped Bi_2WO_6 3D hierarchical microspheres with Mo/W ratio of 0.05 (Fig. 4b), the distortion of lattice fringes inevitablely appeared with the doping of Mo, which means the lower crystallinity of the samples. Therefore, it is reasonable to deduce that the Mo-doping lead to the poorer crystallization of the Bi_2WO_6 3D hierarchical microspheres.

The UV–vis diffuse reflectance spectrum of the Mo-doped Bi_2WO_6 3D hierarchical microspheres is shown in Fig. 5. From the figure, all the samples presented the photoabsorption properties from the UV light region to visible light shorter than 470 nm. The steep shape of the spectrum indicates that the visible light absorption is not due to the transition from the impurity level but due to the band gap transition [22]. For a crystalline semiconductor, the optical band gap was estimated based on their absorption spectra according to the following equation $ahv = A(hv - E_g)^n$, where a, v, E_g, and A are the absorption coefficient, the light frequency, the band gap, and a constant, respectively. n is a coefficient dependent on the type of transition considered: for allowed direct transitions $n = 1/2$ while for allowed indirect transitions $n = 2$. The value of n for Bi_2WO_6 is 2, which means that the optical transition is indirect

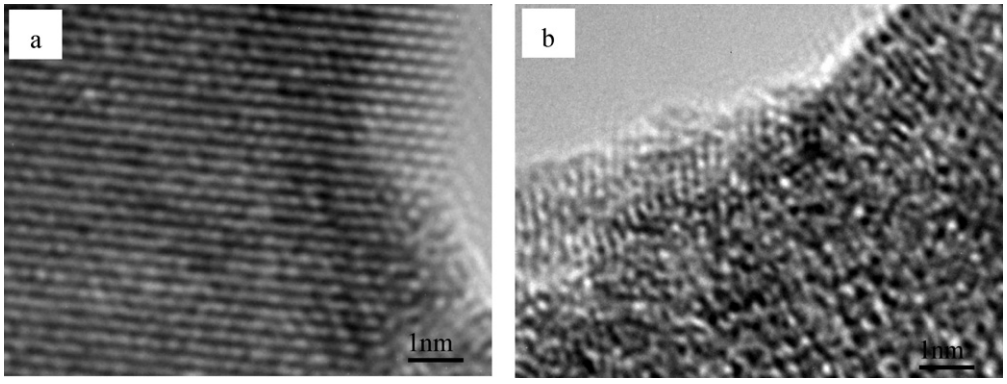

Fig. 4. HRTEM images of the Bi_2WO_6 hierarchical microspheres doped with different contents of molybdenum ions. The doping ratio of Mo/W was 0 (a) and 0.05 (b).

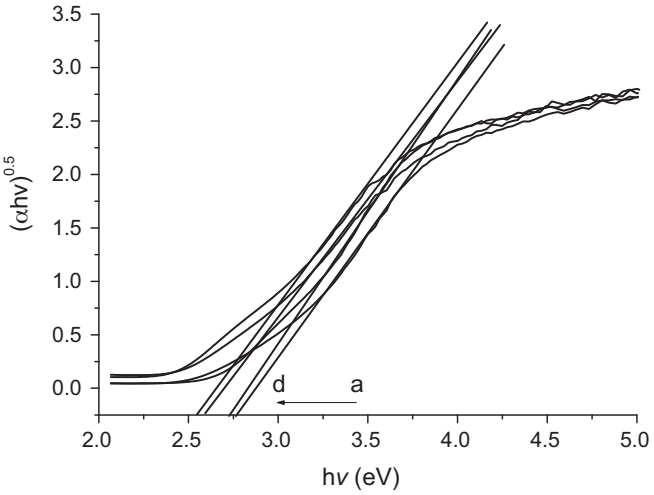

Fig. 6. Indirect band gap determination from the analysis of the absorption spectra of the Bi_2WO_6 hierarchical microspheres doped with different contents of molybdenum ions. From (a)–(d), the doping ratio of Mo/W was 0, 0.02, 0.05 and 0.08, respectively.

allowed [17]. The band gap of the Mo-doped Bi_2WO_6 with different contents of molybdenum ions could be thus estimated to be 2.76 eV, 2.72 eV, 2.59 eV, and 2.55 eV for samples A, B, C, and D, respectively (Fig. 6). Compared with the pure Bi_2WO_6, all Mo-doped Bi_2WO_6 show that with the presence of molybdenum ions, the band gap was decreased. The presence of Mo^{6+} in Bi_2WO_6 does not modify the position of the valence band edge of Bi_2WO_6. Instead, it introduces new energy levels of the molybdenum ions into the band gap of Bi_2WO_6. This band gap decrease might attribute to the charge-transfer transition between Mo^{6+} d electrons and Bi_2WO_6 conduction band.

Rhodamine-B (RhB), a widely used dye, was selected as the model pollutant to evaluate the photocatalytic activity of the Mo-doped Bi_2WO_6 3D hierarchical microspheres. The photocatalytic performances of the Mo-doped Bi_2WO_6 microspheres with different molybdenum contents were determined by comparing the degradation efficiency of RhB (Fig. 7). Among the four samples, the sample C has the highest photocatalytic activity, and the photodegradation efficiency of RhB reached 97% after 60 min of reaction. If plotting $\ln(C/C_0)$ vs irradiation time (t) one can find that the photodegradations of RhB follow the first-order reaction kinetics, i.e. $\ln(C/C_0) = -kt$, with the reaction rate constant (k) = 0.01664, 0.03050, 0.06150 and 0.02991 min^{-1} for Mo-doped Bi_2WO_6 3D hierarchical microspheres photocatalysts with Mo/W ratio of 0, 0.02, 0.05 and 0.08, respectively. The blank experiment with catalyst absence was also performed. It can be found that RhB is almost not decomposed under the same irradiation time. This result clearly indicates that molybdenum ions dopant can effectively improve the photocatalytic degradation activities of Bi_2WO_6 microspheres. When Mo-doping concentration was lower than 0.05, Fig. 7 shows that the degradation rate increases as the increase of molybdenum ions content. However, if Mo-doping concentration further increases, the photocatalytic activity decreases obviously. Surface area is key structural parameter for photocatalysts. It is well known that the photocatalytic activities are closely related to their surface areas [23]. A large surface area are favorable to the photocatalytic performance due to more active sites in the photocatalytic process. The BET surface areas of the pure Bi_2WO_6 and some Mo-doped Bi_2WO_6 are reported in Table 1. It can be observed that the presence of different amounts of Mo species on the samples surface does not influence significantly the value of the BET surface area of Bi_2WO_6 microspheres. This indicates that specific surface area of the sample is not consequentially in association with the photocatalytic activity. The high photocatalytic activity of the sample C is due to the following factors. During the process of photocatalytic reaction, defects can become centers to capture photo-induced electrons, so that the recombination of photo-induced electrons and holes can be effectively inhibited. When the dopant content is more than its optimal value, the defects will be a recombination center. According to the above discussion, the presence of a small amount of molybdenum ions can enhance the activity, but excessive molybdenum ions are detrimental. This may be due to the fact that the molybdenum ions can serve as a mediator of the transfer of interfacial charge at an appropriate doping concentration, and a small amount of molybdenum ions acting as a photo-generated hole and a photo-generated electron trap inhibits the hole-electron recombination. It is also known that the process for photocatalysis of semiconductors is the direct absorption of a photon by band gap of the material and generates electron-hole pairs in the semiconductor particles [24]. The band gap decrease of Mo-doped Bi_2WO_6 photocatalyst

Table 1
BET surface area of the samples prepared at the different Mo-doping concentrations.

Mo-doping concentrations (atomic ratios of Mo–W)	0	0.02	0.05	0.08
Surface area ($m^2\ g^{-1}$)	22.3	21.8	22.5	22.6

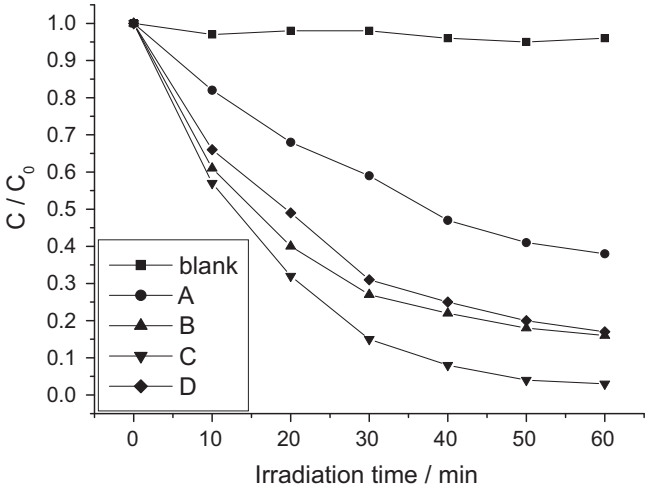

Fig. 7. Photocatalytic degradation of RhB by the Bi_2WO_6 hierarchical microspheres (A–D) with the Mo/W ratio of 0, 0.02, 0.05 and 0.08, respectively.

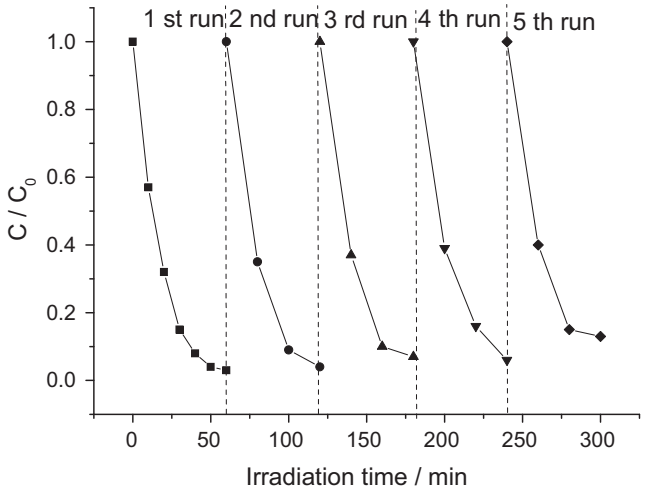

Fig. 8. The lifetime for photodegradation of RhB by sample C.

provides a possibility for enhancing the photocatalytic performance of Bi_2WO_6 microspheres.

The stability of a photocatalyst is important for its application. Herein, the stability of Mo-doped Bi_2WO_6 microspheres (*C*) was investigated. After five recycles for the photodegradation of RhB, the catalyst did not exhibit any significant loss of activity, as shown in Fig. 8, confirming Mo-doped Bi_2WO_6 microspheres (*C*) is not photocorroded during the photocatalytic oxidation of the pollutant molecules.

4. Conclusion

In conclusion, Mo-doped Bi_2WO_6 hierarchical microspheres have been successfully synthesized by a hydrothermal route. The Mo-doped Bi_2WO_6 hierarchical microspheres exhibited the high photocatalytic activity for the decomposition of the aqueous RhB. At an optimal atomic ratio of Mo–W of 0.05, sample has the highest photocatalytic activity, and after 60 min of irradiation, the RhB was removed 97%. Defects and the band gap decreased of Mo-doped Bi_2WO_6 photocatalyst provide a possibility for enhancing the photocatalytic performance of Bi_2WO_6 microspheres. The present work suggests that the idea of using ions doped Bi_2WO_6 could be a strategy to develop an efficient photocatalyst for the destruction of the pollutants.

Acknowledgments

We wish to acknowledge the financial support from the Education Department of Fujian Province (no. JA10071) and Qianjiang Personal Project of Zhejiang Province (no. 2009R10025).

References

[1] Y.M. Xu, C.H. Langfor, UV- or visible-light-induced degradation of X3B on TiO_2 nanoparticles: the influence of adsorption, Langmuir 17 (2001) 897–902.
[2] H.Y. He, J.F. Huang, L.Y. Cao, J.P. Wu, Photodegradation of methyl orange aqueous on $MnWO_4$ powder under different light resources and initial pH, Desalination 252 (2010) 66–70.
[3] K. Honda, A. Fujishima, Electrochemical photolysis of water at a semiconductor electrode, Nature 238 (1972) 37–38.
[4] K. Nagaveni, G. Sivalingam, M.S. Hegde, G. Madras, Solar photocatalytic degradation of dyes: high activity of combustion synthesized nano TiO_2, Appl. Catal. B: Environ. 48 (2004) 83–93.
[5] T. Docters, J.M. Chovelon, J.M. Herrmann, J.P. Deloume, Syntheses of TiO_2 photocatalysts by the molten salts method. Application to the photocatalytic degradation of prosulfuron, Appl. Catal. B: Environ. 50 (2004) 219–226.
[6] A. Maurizio, A. Vincenzo, D.P. Agatino, Preparation, characterization, and photoactivity of polycrystalline nanostructured TiO_2 catalysts, J. Phys. Chem. B 108 (2004) 3303–3310.
[7] M. Andersson, L. Osterlund, S. Ljungstrom, A. Palmqvist, Preparation of nanosize anatase and rutile TiO_2 by hydrothermal treatment of microemulsions and their activity for photocatalytic wet oxidation of phenol, J. Phys. Chem. B 106 (2002) 10674–10679.
[8] D. Ye, D. Li, W. Zhang, M. Sun, Y. Hu, Y. Zhang, X. Fu, A new photocatalyst $CdWO_4$ prepared with a hydrothermal method, J. Phys. Chem. C 112 (2008) 17351–17356.
[9] X.C. Song, E. Yang, R. Ma, H.F. Chen, Z.L. Ye, M. Luo, Hydrothermal preparation and photoluminescence of bundle-like structure of $ZnWO_4$ nanorods, Appl. Phys. A 94 (2009) 185–188.
[10] X.C. Song, E. Yang, R. Ma, H.F. Chen, Y. Zhao, Sodium dodecyl sulfate-assisted synthesis of $CoWO_4$ nanorods, J. Nanopart. Res. 10 (2008) 709–713.
[11] Y. Xing, S. Song, J. Feng, Y. Lei, M. Li, H. Zhang, Microemulsion-mediated solvothermal synthesis and photoluminescent property of 3D flowerlike $MnWO_4$ micro/nanocomposite structure, Solid State Sci. 10 (2008) 1299–1304.
[12] A. Feteira, D.C. Sinclair, Microwave dielectric properties of low firing temperature $Bi_2W_2O_9$ ceramics, J. Am. Ceram. Soc. 91 (2008) 1338–1341.
[13] Y. Shi, S. Feng, C. Cao, Hydrothermal synthesis and characterization of Bi_2MoO_6 and Bi_2WO_6, Mater. Lett. 44 (2000) 215–218.
[14] H. Fu, C. Pan, W. Yao, Y. Zhu, Visible-light-induced degradation of rhodamine B by nanosized Bi_2WO_6, J. Phys. Chem. B 109 (2005) 22432–22439.
[15] Z. Zhang, W. Wang, M. Shang, W. Yin, Low-temperature combustion synthesis of Bi_2WO_6 nanoparticles as a visible-light-driven photocatalyst, J. Hazard. Mater. 177 (2010) 1013–1018.
[16] H. Fu, L. Zhang, W. Yao, Y. Zhu, Photocatalytic properties of nanosized Bi_2WO_6 catalysts synthesized via a hydrothermal process, Appl. Catal. B: Environ. 66 (2006) 100–110.
[17] Z. Cuia, D. Zeng, T. Tang, J. Liu, C. Xie, Processing–structure–property relationships of Bi_2WO_6 nanostructures as visible-light-driven photocatalyst, J. Hazard. Mater. 183 (2010) 211–217.
[18] X.C. Song, Y.F. Zheng, E. Yang, G. Liu, Y. Zhang, H.F. Chen, Y.Y. Zhang, Photocatalytic activities of Cd-doped $ZnWO_4$ nanorods prepared by a hydrothermal process, J. Hazard. Mater. 179 (2010) 1122–1127.
[19] C. Zhang, Y.F. Zhu, Synthesis of square Bi_2WO_6 nanoplates as high-activity visible-light-driven photocatalysts, Chem. Mater. 17 (2005) 3537–3545.
[20] M. Shang, W.Z. Wang, S.M. Sun, L. Zhou, L. Zhang, Bi_2WO_6 nanocrystals with high photocatalytic activities under visible light, J. Phys. Chem. C 112 (2008) 10407–10411.
[21] D. Ma, S. Huang, W. Chen, S. Hu, F. Shi, K. Fan, Self-assembled three-dimensional hierarchical umbilicate Bi_2WO_6 microspheres from nanoplates: controlled synthesis, photocatalytic activities, and wettability, J. Phys. Chem. C 113 (2009) 4369–4374.
[22] A. Kudo, I. Tsuji, H. Kato, $AgInZn_7S_9$ solid solution photocatalyst for H_2 evolution from aqueous solutions under visible light irradiation, Chem. Commun. 17 (2002) 1958–1959.
[23] H. Fu, J. Lin, L. Zhang, Y. Zhu, Photocatalytic activities of a novel $ZnWO_4$ catalyst prepared by a hydrothermal process, Appl. Catal. A: Gen. 306 (2006) 58–67.
[24] X. Li, R. Xiong, G. Wei, Preparation and photocatalytic activity of nanoglued Sn-doped TiO_2, J. Hazard. Mater. 164 (2009) 587–591.